Estimation of Azimuth and Elevation Angles of Ultrasonic Signal Arrival by Indirect Phase Determination

Bogdan Kreczmer(✉)

Department of Cybernetics and Robotics, Electronics Faculty, Wrocław University of Science and Technology, Wrocław, Poland
bogdan.kreczmer@pwr.edu.pl

Abstract. The paper presents the concept of the method of determining the direction of ultrasonic signal arrival, i.e. the azimuth and elevation angles. This method is an extension of the previous approach which was proposed to determine only the azimuth angle. The approach is based on indirect phase determination. This makes it possible to tolerate spacing of receivers greater than half the wavelength of the received signal. At the same time, it provides increased measurement accuracy and reduced hardware requirements. For the proposed method, the preliminary implementation was performed and tested in simulations. This made it possible to estimate the value of the tolerated measurement error.

Keywords: Ultrasonic range finder · Sonar · Direction of arrival

1 Introduction

The main concept of the approach presented in this paper is based on the method described in [2] and in more detail together with the theoretical analysis in [3]. This method makes it possible to construct a 2-D sonar which can determine distance to an object and the azimuth angle of signal arrival. The approach presented in this paper extends this method to the 3-D case when the elevation angle of signal arrival is also estimated (see Fig. 1).

2 Related Work

There are several methods of determining direction of signal arrival (DOA). The well-known method is multiple signal classification (MUSIC) [6]. This method has several variants e.g. root-MUSIC [12], the total spectral search MUSIC method [13], or the partial spectral search one [9]. Another well-known approach to DOA determination is the estimation of signal parameters via rotational invariance techniques (ESPRIT) [4,5]. This approach also has a lot of variants and adaptations e.g. Unitary ESPRIT [1], Conjugate ESPRIT [10].

R. Szewczyk et al. (Eds.): AUTOMATION 2020, AISC 1140, pp. 359–367, 2020.
https://doi.org/10.1007/978-3-030-40971-5_33

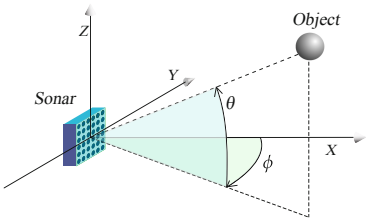

Fig. 1. Object localization by using a sonar which determines its distance, the azimuth angle ϕ and elevation angle θ

Another well-known approach is beamforming which exploits array processing technique. The implementation of such a method is presented in [8]. It appeared to be very effective and made it possible to implement the system BatSLAM which was able to solve the simultaneous localization and mapping problem (SLAM) [7].

The discussed approaches involve methods that are relatively computationally expensive. They important advantage is that they are able to determine the DOA of signals that come from several sources. The approach presented in this paper is restricted to the problem of DOA determination for an echo coming from a single direction. This is the obvious drawback. However, when an emitted signal is short enough, it can be acceptable for many applications of mobile robot navigation. The important advantages are that the computational burden is reduced and the hardware requirements are minimized. Despite this, the implementation of the previous version of the method for the 2-D case has achieved very good accuracy [3].

3 Determining Direction of Signal Arrival

In this paper, it is assumed that the signal emitted, and then received, is narrowband. It is easy to meet this assumption when piezoelectric transducers are used. In this case, to estimate the angle of signal arrival the approach based on measurement of phase shift could be used. This can be done by using receivers arranged on a plain. When the distance between the receivers is less than half the wavelength of the signal, it is sufficient to use three receivers which are placed non-collinear (see Fig. 2). When the distances between receivers are small in relation to the distance of a signal source or object from which it was reflected, the received acoustic wave can be treated as a planewave in the vicinity of the receivers. Assuming t_0, t_1, t_2 are times at which the same planewave was detected by receivers R_0, R_1 and R_2 respectively and $t_0 \leq t_1$ and $t_0 \leq t_2$, distances from receivers R_1 and R_2 to the planewave at the moment when it reached the receiver R_0 are as follows

$$s_1 = v_a \tau_{01}, \qquad s_2 = v_a \tau_{02},$$

where v_a is the speed of acoustic wave, $\tau_{01} = t_1 - t_0$ and $\tau_{02} = t_2 - t_0$. Because the waveplane can be modeled as a plane, it has to meet the equation

$$ax + by + cz + d = 0.$$

where a, b and c are coordinates of the vector perpendicular to the plane. It can be assumed that this vector is normalized. Hereinafter, it will be designated as $\boldsymbol{n} = (n_x, n_y, n_z)$ and

$$n_x^2 + n_y^2 + n_z^2 = 1. \tag{1}$$

Due to the convention of determining azimuth and elevation angle values, it is convenient to assume that the vector $\boldsymbol{n}$ is directed opposite to the direction of wave propagation. In this case, it means that $n_x > 0$ (see Fig. 2). Because the vector $\boldsymbol{n}$ is normalized, the absolute value of d is the distance of the plane to the origin of the coordinate system. The sign of d depends on which side of the plane the origin of the coordinate system is on. But it can be assumed that the origin is located at the receiver R_0 (see Fig. 2). In this case, when the coordinates of a point outside the plane are substituted for the plane equation, d refers to its distance from the plane. Taking it into account the previous discussed assumptions, the coordinates of the receivers R_1 and R_2 are $(0, y_1, z_1)$ and $(0, y_2, z_2)$ respectively, it gives the following set of equations

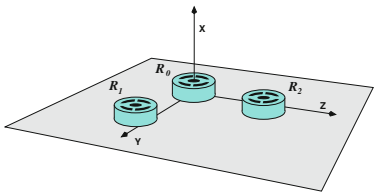

Fig. 2. The coordinate system for the receivers and measurement values interpretation

$$\begin{cases} n_y y_1 + n_z z_1 = s_1, \\ n_y y_2 + n_z z_2 = s_2, \\ n_y^2 + n_z^2 + n_z^2 = 1. \end{cases} \tag{2}$$

Its solution is

$$n_y = \frac{z_2 s_1 - z_1 s_2}{y_1 z_2 - y_2 z_1}, \quad n_z = \frac{y_1 s_2 - y_2 s_1}{y_1 z_2 - y_2 z_1}, \quad n_x = \sqrt{1 - n_y^2 - n_z^2}. \tag{3}$$

Having the coordinates of the normal vector, the azimuth ϕ and elevation θ can be computed using the following formulae

$$\begin{aligned} \phi &= \arcsin \frac{n_y}{\sqrt{n_y^2 + n_x^2}} = \arcsin \frac{n_y}{\sqrt{1 - n_z^2}}, \\ \theta &= \arcsin \frac{n_z}{\sqrt{n_z^2 + n_x^2}} = \arcsin \frac{n_z}{\sqrt{1 - n_y^2}}. \end{aligned} \tag{4}$$

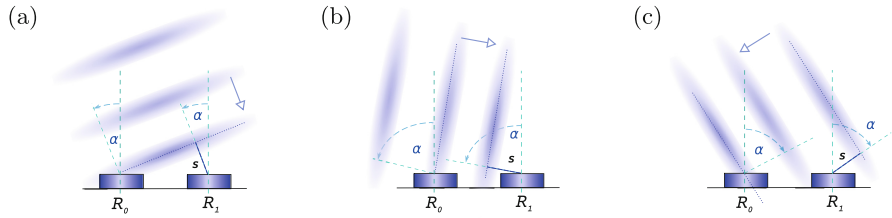

Fig. 3. The same measured distance s can refer to different directions of signal arrival

It is worth noting that due to Eq. (1), it is no need to compute n_x. The azimuth and elevation angles can be determined in this way when the inter-distances between the receivers are less than half the signal wavelength. When they are larger, ambiguity occurs. To explain it, the 2-D case can be considered for simplicity (see Fig. 3). For some angles, after the detection of the wavefront by the R_0 receiver, the receiver R_1 detects a different wavefront than the one that detected by R_0 (compare Fig. 3a and b). When the case presented e.g. in Fig. 3b happens, then the angle α cannot be determined unequivocally. This is because the same distance s refers to different directions of signal arrival. When the wavefront detected by R_0 is not the same as the wavefront detected by R_1, a correction must be added to the measured time $t_{01} = t_1 - t_0$. This correction is a multiple of the signal period T_a and is different for different cases. For example, for the case presented in Fig. 3b it is equal to $1 \cdot T_a$, while for the case presented in Fig. 3c, it is $-2 \cdot T_a$. Considering the 2-D case presented in Fig. 3, the range of possible multiples for the full range $\boldsymbol{\alpha} = [-\frac{\pi}{2}, \frac{\pi}{2}]$ of arrival angles is limited to

$$\mathcal{I}_{\boldsymbol{\alpha}}(b_{01}) = \left[\left\lfloor -\frac{b_{01}}{\lambda} \right\rfloor, \left\lfloor \frac{b_{01}}{\lambda} \right\rfloor \right],$$

where λ is the wavelength of the signal and $\lfloor . \rfloor$ is the floor function. However, due to receivers directivity the range of arrival angles of the signal which can be detected is much smaller than $[-\frac{\pi}{2}, \frac{\pi}{2}]$. Assuming that the range is $\boldsymbol{\alpha} = [\alpha_{min}, \alpha_{max}]$, then the range of possible multiples can be expressed as follows

$$\mathcal{I}_{\boldsymbol{\alpha}}(b_{01}) = \left[\left\lfloor \frac{b_{01} \sin \alpha_{min}}{\lambda} \right\rfloor, \left\lfloor \frac{b_{01} \sin \alpha_{max}}{\lambda} \right\rfloor \right].$$

It enables to construct the set of all possible values of time measurements for the same wavefront detected by R_0 and R_1 that is

$$\boldsymbol{\tau}_{\boldsymbol{\alpha}}(\tau_{01}) = \{\tau_i : \tau_i = \tau_{01} + kT_a, k \in \mathcal{I}_{\boldsymbol{\alpha}}(b_{01}) \wedge |v_a \tau_i| < b_{01}\}.$$

It is worth noting that

$$\forall \tau_i \in \boldsymbol{\tau}_{\boldsymbol{\alpha}}(\tau_j), \quad \boldsymbol{\tau}_{\boldsymbol{\alpha}}(\tau_i) = \boldsymbol{\tau}_{\boldsymbol{\alpha}}(\tau_j).$$

For simplicity, it can be assumed that the directivity pattern of all receivers is the same and has axial symmetry along the receiver acoustic axis. In the same way, it can be created the set $\boldsymbol{\tau_\alpha}(\tau_{02})$ for the second receiver pair of the system $\mathbb{R} = (R_0, R_1, R_2)$ presented in Fig. 2. In this way for this system is obtained

$$\boldsymbol{\tau}^2_{\boldsymbol{\alpha}}(\tau_{01}, \tau_{02}) = \{(\tau_i, \tau_j) : \tau_i \in \boldsymbol{\tau_\alpha}(\tau_{01}) \ \wedge \ \tau_j \in \boldsymbol{\tau_\alpha}(\tau_{02})\}.$$

In the context of Eq. (2), these sets make it possible to create the set of parameters (s_i, s_j)

$$\mathfrak{s}(\tau_{01}, \tau_{02}) = \{(s_i, s_j) : s_i = v_a\tau_i, \tau_i \in \boldsymbol{\tau_\alpha}(\tau_{01}) \ \wedge \ s_j = v_a\tau_j, \tau_j \in \boldsymbol{\tau_\alpha}(\tau_{02})\}$$

In consequence, it determines a set of solutions of Eq. (3),

$$\mathfrak{n}^*(\tau_{01}, \tau_{02}) = \{(n_{x,1}, n_{y,1}, n_{z,1}), \ldots, (n_{x,k}, n_{y,k}, n_{z,k})\}.$$

The measured intervals τ_{01} and τ_{02} are determined by geometry of the receiver system $\mathbb{R}$ and the received signal S. Therefore, for further analysis it will be more convenient to use $\mathbb{R}$ and S as the mapping arguments than the measurement values τ_{01} and τ_{02}. Moreover, due to Eq. (1), to determine angles ϕ and θ, it is enough to know n_y and n_z. Thus, a bit more restricted set $\mathfrak{n}^2$ will be considered further and defined as follows

$$\mathfrak{n}^2(\mathbb{R}, S) = \{(n_{y,1}, n_{z,1}), \ldots, (n_{y,k}, n_{z,k})\}.$$

Having values of $n_{y,i}$ and $n_{y,i}$, then, using Eq. (4) the set of hypothetical signal arrival directions can be created

$$\mathcal{D}(\mathbb{R}, S) = \{(\phi_1, \theta_1), \ldots, (\phi_k, \theta_k)\}.$$

4 Ambiguity Removal

In order to select the proper angles, the 2-D case approach presented in [3] has been adapted. To explain the main idea in the simpler way, the 2-D case will be used again. In this case, it is enough to consider two receiver pairs whose inter-distances are greater than half the wavelength of the signal and they are different. When they receive the same signal, due to ambiguity, two different sets of designated arrival angles are obtained. The only common element is the correct angle of signal arrival (see Fig. 4). Thus, this feature can be exploited for selecting the final solution. To minimize the number of receivers, these two pairs can be integrated in one system consisted of three receivers, using one of the receivers as the common one. It is simple to notice that this approach fails when the inter-distances are the same. Unfortunately, this is not the only case. Therefore, the proper choice of receivers' inter-distances is crucial. A detailed analysis of this approach for the 2-D case is provided in [3]. It should be emphasized that

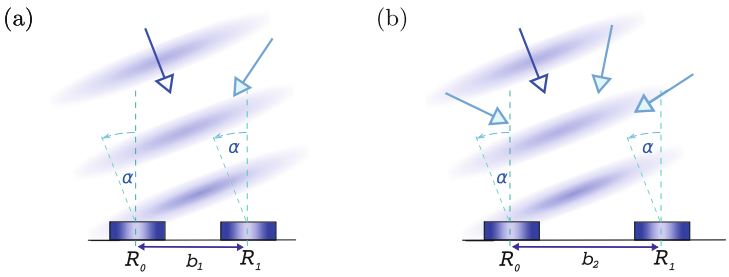

Fig. 4. Examples of possible incident angles for measurement data obtained while the real incident angle is equal to 20°. Directions were determined for the gap size b equal to a – 11 mm, b – 15 mm

this analysis and discussion presented above are true for the narrowband signal. This assumption is met, when popular piezoelectric ultrasonic transducers are used.

The main difference between the 2-D and 3-D cases is that the elementary receiver system has to consist of three receivers instead of two. Moreover, as said before, they cannot be collinear. Following the idea presented for the 2-D case, to apply it to the 3-D case the second receiver system is needed whose inter-distances of receivers are different than in the previous system (see Fig. 5a). Fortunately, these systems can be integrated in a similar way as it was done for the 2-D case. This time, two receivers are the common to both systems (see Fig. 5b). This means that only one additional receiver is needed to follow the approach outlined above. In this way, having the set of transducers $\boldsymbol{R} = \{R_0, R_1, R_2, R_3\}$, two receiver systems can be distinguished, i.e. $\mathbb{R}_1 = \{R_0, R_1, R_2\}$ and $\mathbb{R}_2 = \{R_1, R_2, R_3\}$. However, it is simple to notice, that also two additional systems can be found. In this case, these systems are $\mathbb{R}_3 = \{R_0, R_1, R_3\}$ and $\mathbb{R}_4 = \{R_0, R_2, R_3\}$.

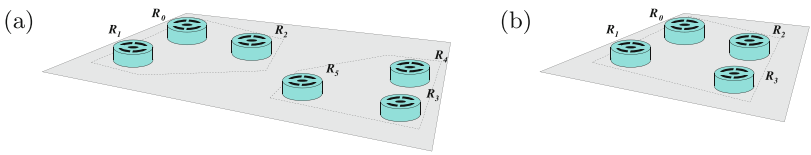

Fig. 5. Receiver system for the 3-D case that makes possible to solve the problem of ambiguity (a) two separate elementary receiver systems, (b) single integrated receiver system

5 Robustness

Because of time measurement errors, values of n_y and n_z are subjects to errors. Assuming that measurement errors of τ intervals can be approximated by the same value $\Delta\tau$ and taking into account (3), then

$$\Delta n_y = \left|\frac{z_1 - z_2}{y_1 z_2 - y_2 z_1}\right| v_a \Delta\tau, \qquad \Delta n_z = \left|\frac{y_2 - y_1}{y_1 z_2 - y_2 z_1}\right| v_a \Delta\tau, \tag{5}$$

It is obvious, but nevertheless it is worth noticing, that for each receiver system $\mathbb{R}_q$ errors of determining coordinates n_y and n_z are constant and strongly depend on the location of its receivers. Taking into account measurement errors, instead of a point set $\mathfrak{n}^2(\mathbb{R}_q, S)$, a set of rectangles is got. It can be defined as follows

$$\mathfrak{n}^2_\Delta(\mathbb{R}_q, S) = \{c_i = [n_{y,i} - \Delta_q n_y, n_{y,i} + \Delta_q n_y] \times [n_{z,i} - \Delta_q n_z, n_{z,i} + \Delta_q n_z] : (n_{y,i}, n_{z,i}) \in \mathfrak{n}^2(\mathbb{R}_q, S)\}$$

Assuming that $(n_{x,S}, n_{y,S}, n_{z,S})$ are the vector coordinates of the direction of the S signal propagation and taking into consideration Eq. (5), a *rectangle of uncertainty* can be obtained

$$c_S = [n_{y,S} - \Delta_q n_y, n_{y,S} + \Delta_q n_y] \times [n_{z,S} - \Delta_q n_z, n_{z,S} + \Delta_q n_z].$$

Following the idea presented in Fig. 4, for the direction n_S the following condition must be met

$$\forall i \in [1, \ldots, n]\ \exists c_i \in \mathfrak{n}^2_\Delta(\mathbb{R}_i, S); \quad c_S \cap \left(\bigcap_{i=1}^{n} c_i\right) \neq \emptyset. \tag{6}$$

The ambiguity is removed when Condition (6) is met only for a single sequence of sets $c_i \in \mathfrak{n}^2_\Delta(\mathbb{R}_i, S)$. Estimating the direction n_S, it is assumed that when only a single sequence of sets $c_i \in \mathfrak{n}^2_\Delta(\mathbb{R}_i, S)$ exits, for which Condition (7) is met,

$$\forall i \in [1, \ldots, n]\ \exists c_i \in \mathfrak{n}^2_\Delta(\mathbb{R}_i, S); \quad \bigcap_{i=1}^{n} c_i \neq \emptyset. \tag{7}$$

then Condition (6) is also met. To estimate values of $n_{y,S}$ and $n_{z,S}$, uncertainty of their determination by subsequent receiver systems has to be taken into account. The uncertainty for $n_{y,i}$ can be defined as follows

$$p_{i,y} = \frac{\sum_{j=1}^{n} \Delta_j n_y - \Delta_i n_y}{(n-1)\sum_{j=1}^{n} \Delta_j n_y}.$$

It is simple noticing that

$$\sum_{i=1}^{n} p_{i,y} = 1.$$

To estimate $n_{y,S}$, a formula can be used

$$\hat{n}_{y,S} = \sum_{i=1}^{n} p_{i,y} n_{y,i}.$$

where $n_{y,i}$ determines c_i which belongs to the sequence of sets meeting Condition (7). In the same way, the value of $n_{z,S}$ can be estimating. Having that, the estimation of ϕ and θ can be computed using Eq. (4).

6 Simulations

At the current stage of work, the preliminary implementation of the method was performed. In tests, the geometry of receivers arrangement presented in Fig. 6a was used. This corresponds to the geometry of the real sonar module which was constructed to implement the method of the 2-D case [3]. However, the geometry of receivers arrangement meets the condition which allows it to be used in the implementation of the method presented in this paper. It was estimated that when $(\phi, \theta) \in [-40°, 40°] \times [-40°, 40°]$, a time measurement error of at least 0.5 µs was correctly tolerated. It means that in this range of error values, ambiguities are successfully removed and the DoA is correctly determined.

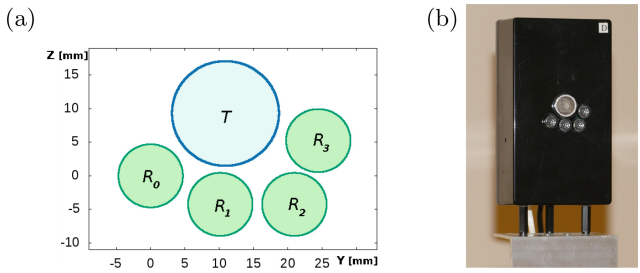

Fig. 6. Geometrical arrangement of sonar receivers and a transmitter (a) dimensioned positions of receivers and a transmitter (b) the real sonar module

7 Conclusion

The presented concept of the method of determining the direction of ultrasonic signal arrival is the extension of the previous version of the method for the 2-D case [3]. The main advantage of a such approach is that using larger inter-distances between receivers, the accuracy of estimation of the signal arrival direction is increased. It can be supposed that this feature will be preserved in extending the method to the 3-D case. At this moment, a preliminary implementation of the method was performed and it was tested in simulation for the

geometry of receivers arrangement of the sonar module used in [3]. It was estimated that a time measurement error of at least 0.5 µs was correctly tolerated. This value is well below expectations. In the case of 2-D, this arrangement of receivers allows obtaining a tolerated measurement error value of up to 1.56 µs. Further examination should make it possible to explain the observed change. This should allow finding a way to increase the value of the tolerated error.

It is worth noting that the field of 3-D ultrasonic sensor construction for robotics is no longer just a field of scientific research. In 2019, Toposens introduced the TS3 sensor [11]. It can be expected that this will promote the use of such sensors in the precise navigation of mobile robots.

References

1. Haardt, M., Nossek, J.A.: Unitary ESPRIT: how to obtain increased estimation accuracy with a reduced computational burden. IEEE Trans. Signal Process. **43**(5), 1232–1242 (1995)
2. Kreczmer, B.: Azimuth angle determination for the arrival direction for an ultrasonic echo signal. J. Autom. Mobile Robot. Intell. Syst. **11**(02), 31–41 (2017)
3. Kreczmer, B.: Estimation of the azimuth angle of the arrival direction for an ultrasonic signal by using indirect determination of the phase shift. Arch. Acoust. **44**(3), 585–601 (2019). http://acoustics.ippt.gov.pl/index.php/aa/article/view/2427
4. Roy, R., Kailath, T.: ESPRIT-estimation of signal parameters via rotational invariance techniques. IEEE Trans. Acoust. Speech Signal Process. **37**(7), 984–995 (1989)
5. Roy, R., Paulraj, A., Kailath, T.: Direction-of-arrival estimation by subspace rotation methods - ESPRIT. In: IEEE International Conference on Acoustics, Speech, and Signal Processing, ICASSP 1986, vol. 11, pp. 2495–2498, April 1986
6. Schmidt, R.: Multiple emitter location and signal parameter estimation. IEEE Trans. Antennas Propag. **34**(3), 276–280 (1986)
7. Steckel, J., Peremans, H.: Spatial sampling strategy for a 3D sonar sensor supporting BatSLAM. In: 2015 IEEE/RSJ International Conference on Intelligent Robots and Systems (IROS), pp. 723–728, September 2015
8. Steckel, J., Peremans, H.: Batslam: simultaneous localization and mapping using biomimetic sonar. PLOS ONE **8**(1), 1–11 (2013)
9. Sun, F., Lan, P., Gao, B.: Partial spectral search-based DOA estimation method for co-prime linear arrays. Electron. Lett. **51**(24), 2053–2055 (2015)
10. Tayem, N., Kwon, H.M.: Conjugate ESPRIT (C-SPRIT). In: IEEE Military Communications Conference, MILCOM 2003, vol. 2, pp. 1155–1160, October 2003
11. Toposens: TS3—3D ultrasonic sensor (2019). https://toposens.com/ts3/#specs
12. Zhang, D., Zhang, Y., Zheng, G., Feng, C., Tang, J.: Improved DOA estimation algorithm for co-prime linear arrays using root-MUSIC algorithm. Electron. Lett. **53**(18), 1277–1279 (2017)
13. Zhou, C., Shi, Z., Gu, Y., Shen, X.: DECOM: DOA estimation with combined MUSIC for coprime array. In: 2013 International Conference on Wireless Communications and Signal Processing, pp. 1–5, October 2013